Exact Stripe, Checkerboard and Droplet Ground States in Two Dimensions

Zsolt Gulácsi[a] and Miklos Gulácsi[b]

[a] *Department of Theoretical Physics,*

University of Debrecen, H-4010 Debrecen, Hungary

[b] *Department of Theoretical Physics, Institute of Advanced Studies,*

Australian National University, ACT 0200 Canberra, Australia

(Dated: February 6, 2008)

Abstract

Exact static non-degenerate stripe and checkerboard ground states are obtained in a two dimensional generalized periodic Anderson model, for a broad concentration range below quarter filling. The random droplet states also present in the degenerate ground state, are eliminated by extending the Hamiltonian with terms of different physical origin such as dimerization, periodic charge displacements, density waves or distortion lines.

I. INTRODUCTION

Quasi-one-dimensional intrinsic inhomogeneities called stripes[1] represent of the most challenging problems in understanding self-organized structures ever since the discovery of high T_c cuprates[2]. Such textures have been observed in other than superconducting cuprates, most notably in manganites[3], nickelates[4] and rare-earth compounds[5]. Most recently it has been shown that all cuprates exhibit intrinsic inhomogeneities in some form or another: checkerboard structures have been identified in lightly hole-doped copper oxides[6], while the electron-doped cuprates show droplet formations[7,8]. These textures are so predominant in high T_cs, that it has been even suggested[9,10] as the best candidate for the electron pairing mechanism in these materials.

After the existence of stripes have been established in a broad spectrum of materials, it becomes clear that they emerge due to a microscopic incompatibility between two phases[2,6,9,10]. However, this interplay not always leads to stripe formations, but could also lead to droplets (or blobs)[7,8] as well. Macroscopic inhomogeneity cannot occur as long as long-range forces are present. But when such forces are absent, depending on doping, local inhomogeneities appear in form of stripes or other form of clustering, e.g., droplets[8,11].

Even thought stripes have been known to exist much before high T_c has been discovered[12], their theoretical understanding lacks rigorous description. Hereafter we want to fill this gap. Hence we present an exact solution of a generalized periodic Anderson model (PAM) with ground states exhibiting intrinsic inhomogeneities of the stripe, checkerboard and droplets type. Using a two band model as a starting point of our analyses it even renders the obtained results to be more generally applicable, since real materials are mostly of multi-band type. These models are usually addressed by projecting the multi-band structure into a few-band picture[13], which we stop for mathematical convenience, at a two band level. However, our study is not a simple two-band model but rather an extended PAM which contains the added feature of strong correlation effects originating from the on-site Coulomb repulsion U present in the correlated (f) band, an arbitrary $U_d > 0$ extra Hubbard interaction in the free (d) band, leaves our results unchanged.

Since stripes and checkerboards are observed in a broad spectrum of materials, we are primarily focusing on ground states which exhibit these inhomogeneities, being less interested in the properties of the homogeneous phases in which they appear.

Our exact results can be summarized as follows. Below quarter filling, two stripe ground states emerge. One (I) with insulating and paramagnetic stripes, while the second one (II) with itinerant and ferromagnetic stripe lines. This second solution allows checkerboard structures as well. In both cases, i.e., I and II, the inter-stripe line regions contain empty sites, hence are insulating. The obtained ground states are in general degenerate. The degeneracy is provided by a random blob structure corresponding to the same energy, the blobs (random shape clusters) possessing the same properties as the stripe lines in cases I and II. The degeneracy of the ground state can however be lifted, the resulting non-degenerate ground state remaining of pure stripe or checkerboard character. The lifting factor we find may have different physical origin as distortion lines, dimerization or periodic charge displacement (density waves). The obtained stripe formation processes are generic and are less sensitive to the properties of the homogenous phases present at quarter filling. We further note that marginal to the stripe problem, but interesting for the PAM itself, we were able to prove rigorously that the studied 2D PAM is ferromagnetic at quarter filling in a restricted region of its parameter space. Similar result has been recently reported for 3D PAM as well[14].

The remaining part of the paper is structured as follows. Sec.II presents the exact transformation of the Hamiltonian in a positive semidefinite form, Sec.III. describes the obtained ground state solutions, Sec.IV. presents a discussion of the obtained results, and Sec.V. concluding the paper, closes the presentation.

II.   THE TRANSFORMATION OF THE HAMILTONIAN

Our starting Hamiltonian is thus, $\hat{H} = \hat{H}_0 + \hat{U}$, written for a free ($d$) and a correlated ($f$) band, where we allow for hopping in both bands:

$$\hat{H}_0 = \sum_{\mathbf{i},\sigma} \left\{ \sum_{\mathbf{r}} \left[\sum_{p=d,f} t_{\mathbf{r}}^p \hat{p}_{\mathbf{i},\sigma}^\dagger \hat{p}_{\mathbf{i}+\mathbf{r},\sigma} + V_{\mathbf{r}}(\hat{d}_{\mathbf{i},\sigma}^\dagger \hat{f}_{\mathbf{i}+\mathbf{r},\sigma} + \right. \right.$$
$$\left. \left. \hat{f}_{\mathbf{i},\sigma}^\dagger \hat{d}_{\mathbf{i}+\mathbf{r},\sigma}) + H.c. \right] + V_0(\hat{d}_{\mathbf{i},\sigma}^\dagger \hat{f}_{\mathbf{i},\sigma} + H.c.) + E_f \hat{n}_{\mathbf{i},\sigma}^f \right\} . \tag{1}$$

To keep the description as general as possible, the above Hamiltonian is defined on a 2D Bravais lattice with unit cell $\mathcal{I}$ and primitive vectors ($\mathbf{x}_1$, $\mathbf{x}_2$). In Eq. (1) $t_{\mathbf{r}}^p$, $V_{\mathbf{r}}$, V_0, and E_f, represent the hopping amplitudes for $p = d, f$ electrons, the non-local and on-site

hybridization, and the local f electron energy, respectively. The coordinate $\mathbf{r}$, with possible values $\mathbf{x}_1, \mathbf{x}_2, \mathbf{x_2} \pm \mathbf{x_1}$, is allowed to extend to *all* sites of $\mathcal{I}$. Within the unit cell $\mathcal{I}_\mathbf{i}$ defined at $\mathbf{i}$, the lattice sites $\mathbf{r}_{\mathcal{I}_\mathbf{i}} = \mathbf{i} + \mathbf{r}_{\alpha\beta}$, with $\mathbf{r}_{\alpha\beta} = \alpha\mathbf{x}_1 + \beta\mathbf{x}_2$, $\alpha, \beta = 0, 1$, can be numbered by $n(\alpha, \beta) = 1 + \alpha + 3\beta - 2\alpha\beta$ without reference to $\mathcal{I}_\mathbf{i}$, see Fig. 1 a). The correlated f band has in addition $\hat{U} = U \sum_\mathbf{i} \hat{n}^f_{\mathbf{i},\uparrow} \hat{n}^f_{\mathbf{i},\downarrow}$, acting on it with $0 < U < \infty$ on-site Hubbard repulsion.

It is known that exact solutions exist mostly in 1D systems and in higher dimensions is almost impossible to find rigorous results. Thus, to find the exact ground state of $\hat{H}$ in 2D we use a method which is based on transforming $\hat{H}$ into a representation which is positive semidefinite. Quantum mechanics tells us that the minimum possible eigenvalue of a positive semidefinite operator, e.g., $\hat{O}$, is zero. Hence the ground state, e.g., $|\Psi_g\rangle$ of $\hat{O}$ can be constructed from $\hat{O}|\Psi_g\rangle = 0$. The fact that ground states containing intrinsic inhomogeneities can be obtained in this manner for a ,,non-integrable"[15] model as 2D-PAM does not come as a surprise, since the applied procedure works even in disordered case[16]. We further note that the method is described in details in Ref. 14 and has been previously used to solve generalized PAM type models at 3/4 filling in 2D[17] and even in 3D[18]. In the present case the transformation is performed in 2D at a lower filling region, which is described in 2D for the first time in this paper.

The transformation proceeds in the following way: first we transform exactly the starting Hamiltonian in a positive semidefinite form. This is accomplished with the use of the operators

$$\hat{A}^\dagger_{\mathbf{i},\sigma} = \sum_{\alpha,\beta=0,1} \sum_{p=d,f} a^*_{n(\alpha,\beta),p} \hat{p}^\dagger_{\mathbf{i}+\mathbf{r}_{\alpha\beta},\sigma}, \tag{2}$$

which are linear combination of the original fermionic operators acting on the corners of an elementary plaquette , see Fig 1 a). It can be easily seen that $\hat{P} = \sum_{\mathbf{i},\sigma} \hat{A}^\dagger_{\mathbf{i},\sigma} \hat{A}_{\mathbf{i},\sigma}$ contains exactly the same operators from Eq. (1). Hence, properly choosing the coefficients $a_{n,p}$, $n = n(\alpha, \beta)$, $\hat{H}_0$ from Eq. (1) can be written as $\hat{H}_0 = \hat{P} + E_g$, where E_g is a constant. The proper mapping is

$$\sum_{j=1}^{l_M} a_{m_j,p} a^*_{n_j,p'} = T^{p,p'}_{\nu,\mathbf{r}}(t^p_\mathbf{r}, t^{p'}_\mathbf{r}, V_\mathbf{r}, E_f), \tag{3}$$

where for the $\mathbf{r} = \alpha_1\mathbf{x}_1 + \alpha_2\mathbf{x}_2$ values allowed by (1), and $p, p' = d, f$, $T^{p,p'}_{\nu,\mathbf{r}}$ is given by

$$T^{p,p'}_{\nu,\mathbf{r}} = (1 - \delta_{\nu,0})[\delta_{p,p'} t^p_\mathbf{r} + (1 - \delta_{p,p'})V_\mathbf{r}] + \delta_{\nu,0}[\delta_{p,p'}(\delta_{p,d}K + \delta_{p,f}(E_f + K)) + (1 - \delta_{p,p'})V_0],$$

4

$$n_j = j\delta_{\nu,0} + (j + |\alpha_1 - \alpha_2|)\delta_{\nu,2} + (\delta_{j,2} + (4|\alpha_1| + 2|\alpha_2|)\delta_{j,1})\delta_{\nu,1},$$

$$m_j - n_j = 2\delta_{\nu,2} + \delta_{\nu,1}[7 - 4j + (6j - 10)|\alpha_1| + (6j - 8)|\alpha_2|].$$

$$2l_M = 8 - 5\nu + \nu^2, \quad \nu = (|\alpha_1| + |\alpha_2|). \tag{4}$$

Furthermore, $E_g = -KN$, where N is the number of electrons, and $K = \sum_{n=1}^{4} |a_{n,d}|^2$. Consequently, the starting Hamiltonian, $\hat{H}$, becomes positive semidefinite

$$\hat{H} = \hat{P} + \hat{U} + E_g, \tag{5}$$

except the additive constant E_g. The transformation of the starting Hamiltonian based on the plaquette operators from Eq. (2) into Eq.(5) is possible only if Eq.(3) containing 19 non-linear coupled equations allows solutions for the $a_{n,p}$ parameters. The different type of solutions of these non-linear equations are presented in the following.

III. GROUND STATE SOLUTIONS

We found that there are two types of solutions which satisfy the system of non-linear equations (3). These two types of solutions will be denoted by $R = I$ and $R = II$. In I, for $a_{n,d}^*/a_{n,f}^* = q_n = q = $ real for all n, $\hat{A}_{\mathbf{i},\sigma}$ reduces to one-site form $\hat{A}_{\mathbf{i},\sigma} = \sum_{n=1}^{4} a_{n,d}\hat{\mathcal{A}}_{\mathbf{i}+\mathbf{r}_n,\sigma}$, $\hat{\mathcal{A}}_{\mathbf{i},\sigma} = \hat{d}_{\mathbf{i},\sigma} + \hat{f}_{\mathbf{i},\sigma}$ for all $\mathbf{i}$. While in II, $q_n \neq q = $ real, and such a reduction of $\hat{A}_{\mathbf{i},\sigma}$ into $\hat{\mathcal{A}}_{\mathbf{i},\sigma}$ is not possible.

In the following we will analyze in details the ground state corresponding to the solutions I and II: (A) We first determine the homogeneous phases at quarter filling ($N = N_\Lambda$, N_Λ being the number of lattice sites). (B) By decreasing N we find degenerated droplet, stripe and checkerboard ground states which we will present in detail, and (C) extensions of $\hat{H}$ are identified to lift the degeneracy leading to pure, non-degenerate stripe and checkerboard ground states.

A. Ground states at quarter filling

To find the ground state at quarter filling, a *complementary* unit cell operator[14] $\hat{B}_{\mathbf{i},\sigma}$ is defined by

$$\{\hat{A}_{\mathbf{i},\sigma}, \hat{B}_{\mathbf{i}',\sigma'}^\dagger\} = 0, \quad \forall \mathbf{i}, \mathbf{i}', \sigma, \sigma'. \tag{6}$$

For case II, $\hat{B}_{\mathbf{i},\sigma} = \sum_{\alpha,\beta=0,1} \sum_{p=d,f} b_{n,p}\hat{p}^{\dagger}_{\mathbf{i}+\mathbf{r}_n,\sigma}$, [as shown in Fig. 1 b)], and defining $n'(\alpha,\beta) = 3 + \alpha - \beta - 2\alpha\beta$, and taking $w = b_{1,d}/a^{*}_{3,f}$, one finds

$$b_{n,f} = -wa^{*}_{n',d}, \quad b_{n,d} = +wa^{*}_{n',f} . \tag{7}$$

While, for case I, $\hat{B}_{\mathbf{i},\sigma} = \sum_{n=1}^{4} b_{n,d}\hat{\mathcal{B}}_{\mathbf{i}+\mathbf{r}_n,\sigma}$, and $\{\hat{\mathcal{A}}_{\mathbf{i},\sigma}, \hat{\mathcal{B}}^{\dagger}_{\mathbf{i}',\sigma'}\} = 0$, $\hat{\mathcal{B}}_{\mathbf{i},\sigma} = \hat{d}_{\mathbf{i},\sigma} - \hat{f}_{\mathbf{i},\sigma}$ holds.

Introducing $\hat{D}^{\dagger}_{\mathbf{i},\sigma}(R) = (\hat{\mathcal{C}}^{\dagger}_{\mathbf{i},\sigma}\delta_{R,I} + \hat{B}^{\dagger}_{\mathbf{i},\sigma}\delta_{R,II})$, where $\hat{\mathcal{C}}_{\mathbf{i},\sigma} = (\hat{\mathcal{B}}^{\dagger}_{\mathbf{i},\sigma} + v_{\mathbf{i}}\hat{\mathcal{B}}^{\dagger}_{\mathbf{i},-\sigma})$ and $v_{\mathbf{i}}$ are arbitrary coefficients, the exact ground state at quarter filling becomes

$$|\Psi_{g,R,1/4}\rangle = \prod_{\mathbf{i}=1}^{N_{\Lambda}} \hat{D}^{\dagger}_{\mathbf{i},\sigma}(R)|0\rangle , \quad R = I, II \tag{8}$$

where $|0\rangle$ is the bare vacuum. This is the ground state wave function, i.e., $(\hat{P}+\hat{U})|\Psi_{g,R,1/4}\rangle = 0$. Here $\hat{U}|\Psi_{g,R,1/4}\rangle = 0$ since, for $R = I$ the electrons with arbitrary spins are introduced on different sites, and for $R = II$ all $\hat{B}^{\dagger}_{\mathbf{i},\sigma}$ in (8) have the same fixed spin σ, so the double occupancy for both p is excluded. Besides, based on (6), further we have $\hat{P}|\Psi_{g,R,1/4}\rangle = 0$. Since the minimum eigenvalue of $\hat{P} + \hat{U}$ is zero, thus $|\Psi_{g,R,1/4}\rangle$ is the ground state for non-zero, positive, although arbitrary U. The ground state for case I is degenerate and globally paramagnetic, with one electron on each site, i.e. the state is localized. While in case II the ground state is non-degenerate, is a saturated ferromagnet, with 0, 1, or 2 electrons on any $\mathbf{i}$ site, e.g. the state is itinerant.

B. Ground states below quarter filling

1. Random droplet ground states

Decreasing the number of $\hat{D}^{\dagger}_{\mathbf{i},\sigma}$ operators in the product of Eq.(8), the exact ground state below quarter filling can be written as well. In case I, for $N < N_{\Lambda}$, we obtain

$$|\Psi_{g,I,1/4\geq n>0}\rangle = \prod_{\mathbf{i}=1}^{N} \hat{\mathcal{C}}^{\dagger}_{\mathbf{i},\sigma}|0\rangle , \tag{9}$$

where sites $\mathbf{i}$ can be arbitrarily chosen. Being empty sites present, the ground state is an itinerant paramagnetic phase. In case II, the ground state is reached only if touching $\hat{B}^{\dagger}_{\mathbf{i},\sigma}$ operators defined on different sites [for example $(\hat{B}_{19,\sigma}, \hat{B}_{25,\sigma})$ in Fig. 2 a)] have the same spin in order to maintain the $\hat{U}|\Psi_g\rangle = 0$ condition. These neighboring $\hat{B}^{\dagger}_{\mathbf{i},\sigma}$ operators with fixed spin build up different blocks (droplets) Bl_j containing N_{Bl_j} particles. Two different

blocks have no common lattice sites, and their spin is non-correlated. If we denote by N_{Bl} the number of blocks, then the ground state wave function becomes

$$|\Psi_{g,II,1/4 \geq n>0}\rangle = \prod_{j=1}^{N_{Bl}} \left(\prod_{\mathbf{i}=1}^{N_{Bl_j}} \hat{B}_{\mathbf{i},\sigma_j}^{\dagger} \right) |0\rangle , \qquad (10)$$

where $\sum_j N_{Bl_j} = N$, but otherwise, N_{Bl_j} and the shape of the blocks remain arbitrary, as on the example shown in Fig. 2 b). This state is itinerant and represents a fully saturated ferromagnet up to $N \geq N_\Lambda - 8$. In the limit $N = N_\Lambda - 8$ there is always a possibility for a new block to appear on the lattice, in a way that is not in contact with other blocks and as such it can have opposite spin. For example, in Fig. 2 a), the middle block $B_{15,\downarrow}$ is isolated and has opposite spin compared to the big block surrounding it. Hence, for $N < N_\Lambda - 8$ the ground state is not anymore fully saturated. Further decreasing N, the ground state remains ferromagnetic[19] until two disjoint blocks with the same number of sites but opposite spins can be constructed. This happens at $N_p^c = N_\Lambda - 2L$, where $N_\Lambda = L \times L$. Thus, for $N < N_p^c$, the ground state is globally paramagnetic.

2. Degenerated stripe ground state solutions

Decreasing N below N_p^c, stripes emerge in the ground state in both Eqs. (9,10) as vertical stripes (Fig. 3) or diagonal stripes (Fig. 4). The ground state wave function containing N_{St} vertical stripe lines is

$$|\Psi_{g,R,I_{St}}\rangle = \prod_{j=1}^{N_{St}} (\prod_{\mathbf{i} \in I_{St,j}} \hat{D}_{\mathbf{i},\sigma_j}^{\dagger})|0\rangle , \qquad (11)$$

where $I_{St,j}$ in case I (II) represents the stripe line j (plaquette stripe column j), and $I_{St} = \sum_j I_{St,j}$. For example, from (11), the vertical stripes are obtained in case I (II) by a displacement along periodic vertical lines (vertically constructed plaquette columns) of $\hat{\mathcal{C}}_{\mathbf{i},\sigma}^{\dagger}$ ($\hat{B}_{\mathbf{i},\sigma}^{\dagger}$) operators. In Fig. 3 a) case I is shown with column stripes, while Fig. 3 b) depicts case II with plaquette columns. For diagonal stripes, the vertical displacement must be changed to diagonal one, as shown in Fig. 4. In the case II at $d1 = d2$, see Fig. 5, the stripe structure turns into a checkerboard one. The stripe lines for case I are paramagnetic and insulating, while they are itinerant and ferromagnetic for case II. Different stripe lines which are not in contact have non-correlated spin.

C. Non-degenerated stripe and checkerboard ground states

For $N < N_p^c$, droplet [see Fig. 2 b)] and stripe solutions coexist as the ground state is degenerate. However, the droplet contributions can be eliminated in exact terms from the ground state by adding new Hamiltonian contributions to $\hat{H}$. For example, let us consider $\hat{H}_A = -|W_1| \sum_{\mathbf{i} \in I_{St}} \hat{n}_\mathbf{i}$, where $\hat{n}_\mathbf{i} = \sum_{\sigma,p} \hat{n}_{\mathbf{i},\sigma}^p$. If I'_{St} contains all lattice sites from $\hat{\mathcal{D}}_{I'_{St}}^\dagger = \prod_{j=1}^N \hat{D}_{\mathbf{i}_j,\sigma_j}$ and $I_{St} = I'_{St}$ holds, then $[\sum_{\mathbf{i} \in I_{St}} \hat{n}_\mathbf{i}] \hat{\mathcal{D}}_{I'_{St}}^\dagger = \hat{\mathcal{D}}_{I'_{St}}^\dagger [N + \sum_{\mathbf{i} \in I_{St}} \hat{n}_\mathbf{i}]$ provides the minimum possible eigenvalue for $\hat{H}_A$ via $\hat{H}_A |\Psi_{g,R,I_{St}}\rangle = -|W_1| N |\Psi_{g,R,I_{St}}\rangle$. If however, $I'_{St} \neq I_{St}$ [for example, if $\mathbf{j}_2$ moves to the in $\mathbf{j}_1$ position, Fig. 3 a)], then $|\Psi_{g,R,I_{St}}\rangle$ is not anymore an eigenstate of $\hat{H}_A$. Consequently, $|\Psi_{g,R,I_{St}}\rangle$ becomes the unique, non-degenerate ground state of $\hat{H} + \hat{H}_A$. If we add to $\hat{H}_A$ the term $\hat{H}'_A = |W_2| \sum_{\mathbf{i} \notin I_{St}} \hat{n}_\mathbf{i}$, as well, the results remain unchanged. A Hamiltonian term of the form $\hat{H}_A$ is motivated in case of cuprates by low temperature tetragonal fluctuations[20]. The potential W in $\hat{\bar{H}}_A = \hat{H}_A + \hat{H}'_A$ can be generated by a periodic charge displacement or charge density wave (see Fig. 7), which is able to stabilize a stripe phase. Such a behavior has been already seen[22] in cuprates. Similarly, the checkerboard state also can be made stable[21]. A checkerboard is obtained, for example in Fig. 4 b), if we take $d1 = d2 = 2$. This is stabilized by a Hamiltonian term $\hat{H}_A$, which has a set of lattice sites I_{St}, in such a way that it contains only next-nearest-neighbor sites on each second diagonal.

Furthermore, the vertical stripes from Fig. 3 b), will be stabilized by a dimerization term of the form $\hat{H}_B = \sum_\sigma \sum_{\mathbf{i} \in I_E} \hat{E}_{\mathbf{i},\sigma}^\dagger \hat{E}_{\mathbf{i},\sigma}$, $\hat{E}_{\mathbf{i},\sigma} = \sum_{p=d,f} (e_{1,p} \hat{p}_{\mathbf{i},\sigma} + e_{2,p} \hat{p}_{\mathbf{i}+\mathbf{x}_1,\sigma})$, where I_E contains only each second site of horizontal lattice rows[23], see Fig. 6. For $\hat{H}_B$ described in Ref. 23, the stable stripe phase occurs above the surface presented in Fig. 8. Modifying I_E, other stripes can be addressed as well. The important effect of dimerization on stripes stabilization have been recently shown using numerical simulations[24].

IV. DISCUSSION OF THE RESULTS

The obtained inhomogeneities are not connected in principle neither to certain special values of the parameters, nor to special properties of the homogeneous phases present at quarter filling. In the following we present several remarks to support this and in closing the obtained stripe formation process is summarized.

Firstly, for a given Hamiltonian, a given decomposition in positive semidefinite operators at a given filling factor is not unique[14,25,26]. The decomposition itself can be done in several different ways, leading to different $\hat{A}_{\mathbf{i},\sigma}$ operators, different matching conditions, hence different interdependencies between microscopic parameters obtained during the solution of the matching conditions (i.e. equations of the type (3)), providing similar solutions, and similar characteristics in different regions of the parameter space. For example, as shown in Ref.[25], instead of plaquettes, rhombi can also be used in defining $\hat{A}_{\mathbf{i},\sigma}$, obtaining the same type of solutions, but in other regions of the parameter space. Other possibilities are to simply tilt the unit cell[14], or to decompose in $\sum_{\mathbf{i}} \hat{A}_{\mathbf{i}}^{\dagger} \hat{A}_{\mathbf{i}}$, where $\hat{A}_{\mathbf{i}} = \sum_{\sigma} \hat{A}_{\mathbf{i},\sigma}$, as described in Ref.[26], etc.

Secondly, the different solutions of the matching conditions all give homogeneous phase at quarter filling. Stripes will appear from each of these homogeneous phases with (hole) doping. This can be easily understood from the observation that the $\hat{B}_{\mathbf{i},\sigma}$ (or $\hat{\mathcal{B}}_{\mathbf{i},\sigma}$) operators which are characteristic of the stripe ground state, see eg, Eqs.(6,7), can appear for arbitrary $\hat{A}_{\mathbf{i},\sigma}$. Consequently, the obtained stripe formation process is weakly dependent on the properties of the homogeneous phase from which the stripes emerge.

Thirdly, each homogenous phase (and hence each stripe structure originating from it) appears for different, well-defined conditions. For example, see also Ref.[19], stripes with ferromagnetic and itinerant stripe lines can be obtained from the itinerant ferromagnetic homogenous phase when the one particle part of the Hamiltonian in (1) has such parameters that $\hat{H}_0$ will have a diagonalized partially filled lower flat band. One the other hand, insulating paramagnetic stripe lines are obtained in a different parameter space region, where localized homogenous phase can occur, etc.

Fourthly, an additional repulsive Hubbard term acting in the d-band will not change the obtained results. Consequently, the obtained ground states and inhomogeneities are valid not only in the 2D PAM, but also in a more general 2D two-band Hubbard model as well.

Lastly, in our rigorous description we obtained a non-degenerate ground state exhibiting stripe structure in the following steps: we doped the homogeneous phase at quarter filling. This resulted in a degenerate ground state to appear, which contained both random droplets and stripe solutions. In the last step we lifted the degeneracy by adding a so-called stabilization term to the Hamiltonian. By doing this we eliminated the random droplets from the degenerated ground state, obtaining providing a non-degenerated stripe ground state

solution.

V. CONCLUSIONS

In conclusion, providing exact results for stripe, checkerboard vs. droplet interplay, we show how such intrinsic inhomogeneities appear in a 2D Hamiltonian as a non-degenerate ground states. For this, 1) a generalized PAM is used and cast in a positive semidefinite form, 2) the ground states are explicitly constructed at and below quarter filling, and 3) the ground state degeneracy provided by random droplets is eliminated using extension terms representing, e.g., distortion lines, dimerization or density waves. The inhomogeneities were shown to exist in a broad concentration range below quarter filling and they are either (case I) paramagnetic and localized, or (case II) itinerant and ferromagnetic. In both of these cases the inter-stripe lines are insulating. As has been underlined, stripes can emerge from different homogeneous phases so are less sensitive to microscopic parameters of $\hat{H}$. As marginal for the stripes, but important for PAM we derive an exact ferromagnetic ground state, as well, in $2D$ at quarter filling. An extra Hubbard interaction in the d band, $U_d > 0$ leaves the above results unchanged. The presented positive semidefinite decomposition is not unique, can be effectuated in several ways, leading to similar results also in other regions of the parameter space.

---

[1] J. Zaanen and O. Gunnarson, Phys. Rev. **B40**, 7391 (1989).

[2] S. A. Kivelson, I. P. Bindloss, E. Fradkin, V. Oqanesyan, J. M. Tranquada, A. Kapitulnik, C. Howald, Rev. Mod. Phys. **75**, 1201 (2003).

[3] M. B. Salamon and M. Jaime, Rev. Mod. Phys. **73**, 583 (2001)

[4] J. Q. Yan, J. S. Zhou and J. B. Goodenough, Phys. Rev. **B68**, 104520 (2003)

[5] R. G. Stewart, Rev. Mod. Phys. **73**, 797 (2001)

[6] T. Hanaguri, C. Lupien, Y. Kohsaka, D. H. Lee, M. Azuma, M. Takano, H. Takagi and J. C. Davis, Nature **430**, 1001 (2004).

[7] O. N. Bakharev, I. M. Abu-Shiekah, H. B. Brom, A. A. Nuqroho, I. P. McCulloch and J. Zaanen, Phys. Rev. Lett. **93**, 37002 (2004).

[8] D. H. Lee and S. A. Kivelson, Phys. Rev. **B67**, 024506 (2003).

[9] S. M. Hayden, H. A. Mook, P. Dai, T. G. Perring and F. Dogan, Nature **429**, 531 (2004).

[10] J. M. Tranquada, H. Woo, T. G. Perring, H. Goka, G. D. Gu, G. Xu, M. Fujita and K. Yamada, Nature **429**, 534 (2004).

[11] U. Löw, V. J. Emery, K. Fabricius, and S. A. Kivelson, Phys. Rev. Lett. **72**, 1918 (1994)

[12] E. L. Nagaev, Usp. Fiz. Nauk 166, 833 (1996), Engl. trans. Phys. Usp. 39, 781 (1996).

[13] M. Kollar, R. Strack, and D. Vollhardt, Phys. Rev. **B53**, 9225, (1996).

[14] Z. Gulácsi, D. Vollhardt, Phys. Rev. **B72**, 075130, (2005).

[15] In special cases called ,,integrable" (i.e. the number of degrees of freedom is equal to the number of constants of motion), the whole spectrum can be deduced using methods as Bethe Ansatz. In our case, only the ground state is obtained.

[16] Z. Gulácsi, Phys. Rev. **B69**, 054204, (2004).

[17] P. Gurin and Z. Gulácsi, Phys. Rev. **64**, 045118, (2001); Z. Gulácsi, Phys. Rev. **B66**, 165109 (2002);

[18] Z. Gulácsi and D. Vollhardt, Phys. Rev. Lett. **91**, 186401 (2003).

[19] Eq.(3) shows that when ferromagnetism emerges, the diagonalized $\hat{H}_0$ has a partially filled lower flat band.

[20] Y. Shiba, T. Tohyama and S. Maekawa, Phys. Rev. **B64**,054519,(2001).

[21] S. R. White and D. J. Scalapino, cond-mat/0408249.

[22] J.M.Tranquada, J. D. Axe, N. Ichikawa, A. R. Moodenbaugh, Y. Nakamura and S. Uchida, Phys. Rev. Lett. **78**,338,(1997).

[23] We must consider $\hat{B}_{\mathbf{i},\sigma} = \hat{B}^{h,1}_{\mathbf{i},\sigma} + \hat{B}^{h,2}_{\mathbf{i}+\mathbf{x_2},\sigma}$, where $\hat{B}^{h,l}_{\mathbf{i},\sigma} = \sum_{p=d,f}(b_{3l-2,p}\hat{p}_{\mathbf{i},\sigma} + b_{l+1,p}\hat{p}_{\mathbf{i}+\mathbf{x_1},\sigma})$, as shown in Fig. 1 b), and $\{\hat{E}_{\mathbf{i},\sigma}, B^{\hat{h},l}_{\mathbf{i}',\sigma'}^{\dagger}\} = 0$, $l = 1, 2$, $\mathbf{i}, \mathbf{i}' \in I_E$. At $e_{i,f} = 0$, we have active $\hat{H}_B$ for $|t^f_{x+y}| = |t^f_{y-x}|$, obtaining $\hat{E}_{i,\sigma} = e_{i,d}(\hat{d}_{i,\sigma} - \hat{d}_{i+1,\sigma})$ for all even i in every lattice row with arbitrary $e_{i=even,d} = e_d$, and $e_{i=odd,d} = 0$.

[24] K. H. Ahn, T. Lookman and A. R. Bishop, Nature **428**, 401 (2004).

[25] Z. Gulácsi, Eur. Phys. J. **B30**, 295 (2002).
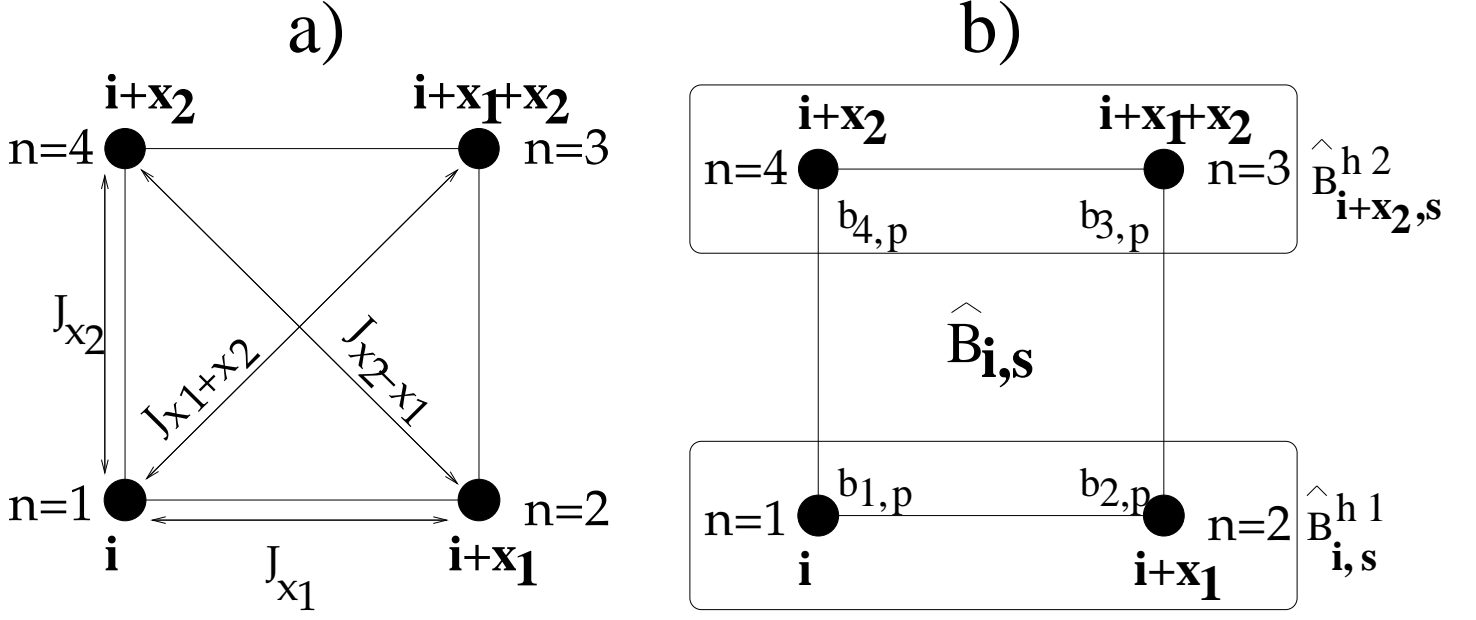
[26] Z. Gulácsi, Phys. Rev. **B66**, 165109, (2002).

FIG. 1: a)Unit cell ($\mathcal{I}$), and, b) the $\hat{B}_{\mathbf{i},s}$ operator defined at an arbitrary site $\mathbf{i}$, $\mathbf{x}_\tau$ are the primitive vectors and n is the $\mathbf{i}$ independent notation of the sites in $\mathcal{I}_{\mathbf{i}}$. For a) arrows indicate hopping and hybridization matrix elements (J=t, V). In b), the $b_{n,p}$, $p = d, f$ coefficients are shown together with a decomposition in horizontal components $\hat{B}_{\mathbf{i},s} = \hat{B}_{\mathbf{i},s}^{h1} + \hat{B}_{\mathbf{i}+\mathbf{x}_2,s}^{h2}$ of the complementary operator $\hat{B}_{\mathbf{i},s}$.
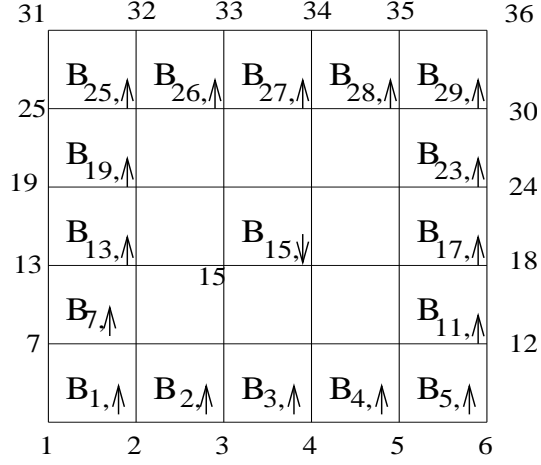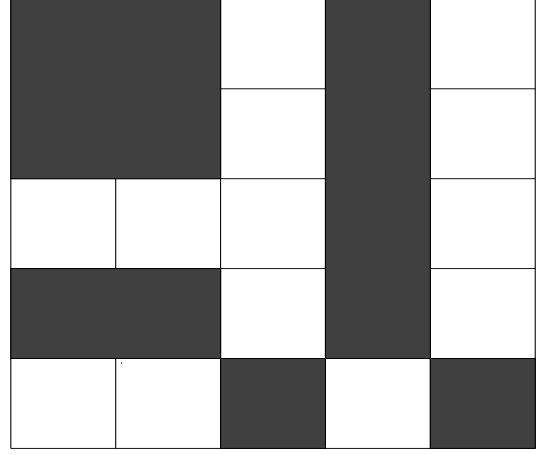
FIG. 2: (a) Isolated plaquette with opposite spin at site $i = 15$, and (b) droplet solutions for case II. The blocks $B_{i,\sigma}$ introducing the $\hat{B}^{\dagger}_{i,\sigma}$ operators in the ground state wave-function of case II are presented as shaded plaquettes in b).
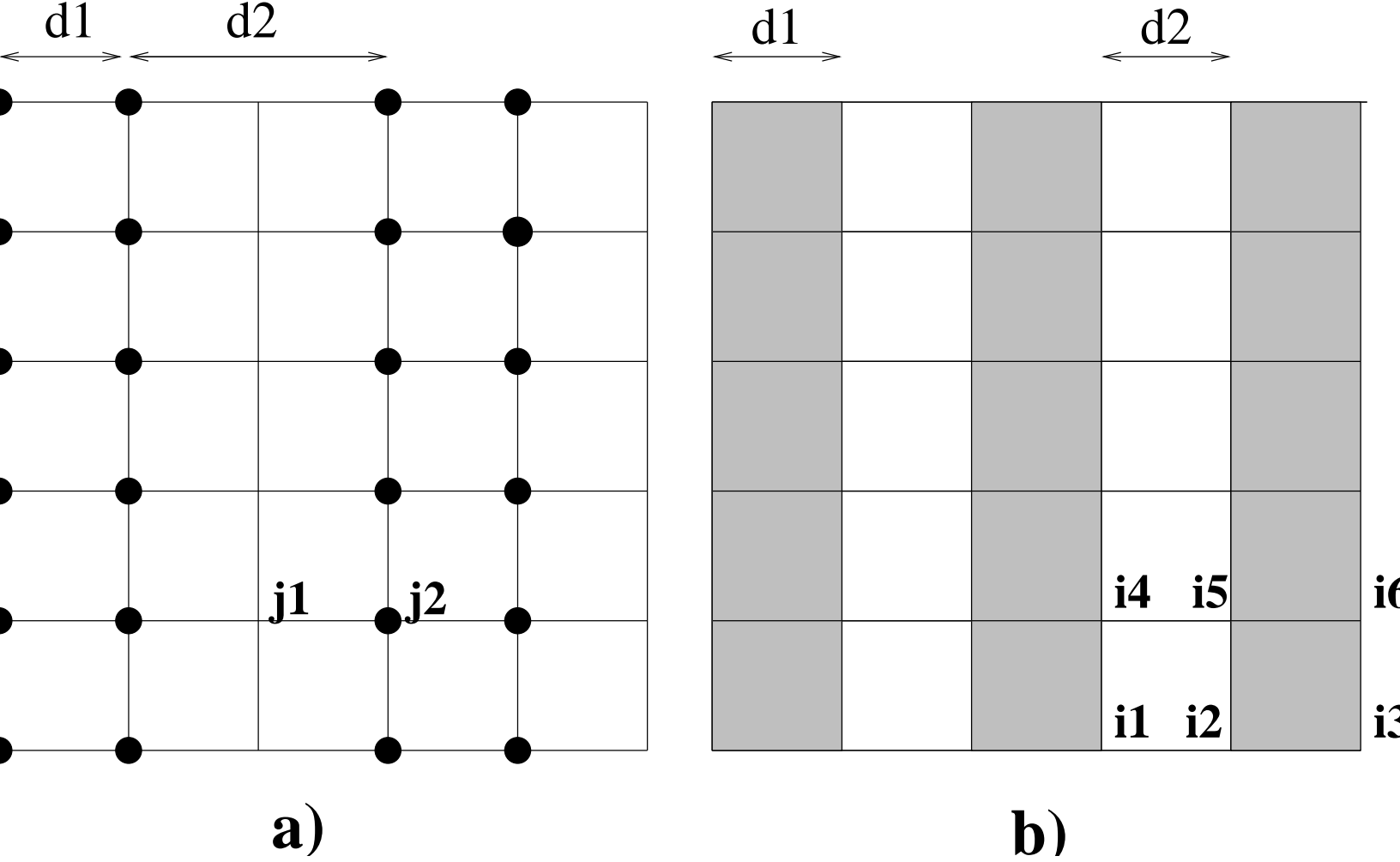
FIG. 3: Example of vertical stripe solutions for case I shown in (a) and II in (b). For a) (or b)) full circles (or shaded plaquettes) denote sites (or unit cells) whose $\hat{\mathcal{C}}^{\dagger}_{\mathbf{i},\sigma}$ (or $\hat{B}^{\dagger}_{\mathbf{i},\sigma}$) contribution is in the ground state wave-function Eq.(8). For example, site $j2$ in case I (unit cell (i2,i3,i5,i6) in case II). In both cases $d1$ ($d2$) represents a measure of the stripe line width (inter stripe line distance) in x direction and $|\mathbf{x}_1|$ units.
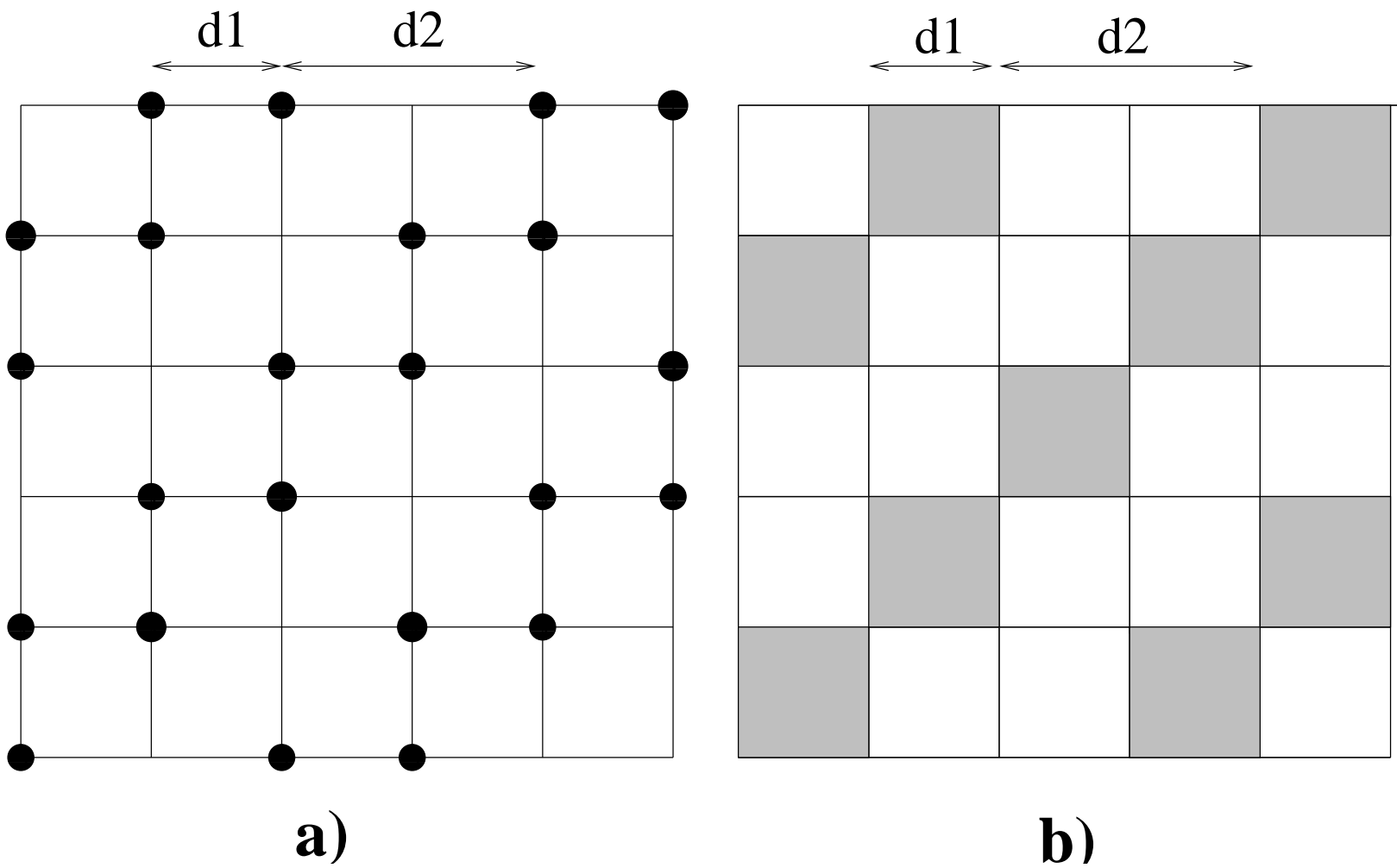
FIG. 4: Example of diagonal stripe solutions for case I shown in (a) and case II in (b). Notations are as in Fig.3.
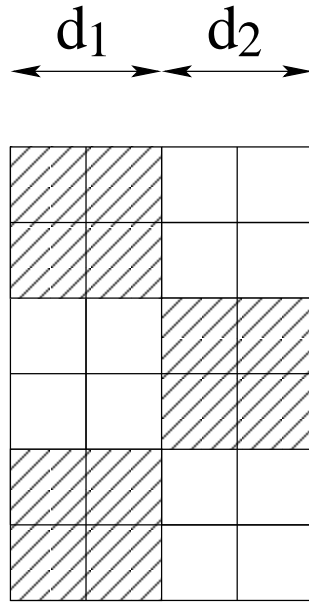
FIG. 5: Checkerboard originating from diagonal stripes at $d_1 = d_2$, see also Fig.4.b)

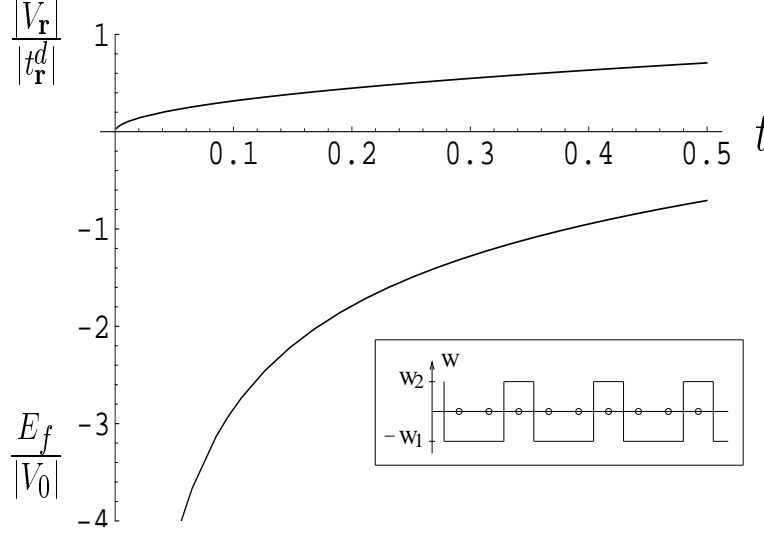FIG. 6: Bond alternation in x-direction to stabilize the stripes from Fig. 3 b), $J_x = t_x^p, V_x$.

FIG. 7: $\hat{H}_0$ parameters for case I vs. $t = t_{\mathbf{x}_\tau}^f/t_{\mathbf{x}_\tau}^d$, at $(t_x^d)^2, (t_y^d)^2 \geq 4t_{x+y}^d t_{y-x}^d$. The inset shows the potential W created by $\hat{\tilde{H}}_A$ acting on the charge degrees of freedom in x direction stabilizing the stripes from Fig.3 a).
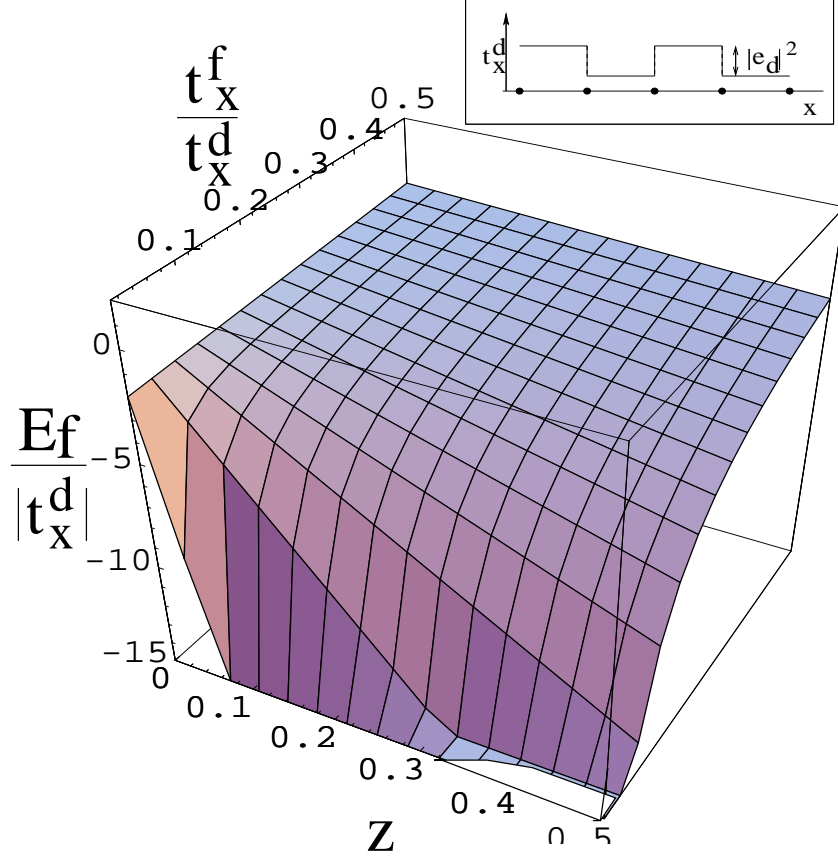
FIG. 8: (Color online) The $E_f/|t_x^d|$ surface in function of $t = t_x^f/t_x^d$ and the anisotropy parameter $z = (|t_y^f| - |t_x^f|)/|t_x^d|$ above which the $R = II$ stripe ground-state from Fig.3.b emerge stabilized by $\hat{H}_B$ in conditions from Ref.[23]. For hybridization $V_x = V_0 = 0$, and for other $\mathbf{r}$, $|V_\mathbf{r}|/|t_\mathbf{r}^f| = \sqrt{|t|}$ holds. The inset shows the required t_x^d alternation introduced by $\hat{H}_B$. For $\hat{H}_B = 0$, FM is present on the plotted surface at 1/4 filling.